

## A DYNAMICAL SIGNATURE OF MULTIPLE STELLAR POPULATIONS IN 47 TUCANAE

HARVEY B. RICHER<sup>1</sup>, JEREMY HEYL<sup>1</sup>, JAY ANDERSON<sup>2</sup>, JASON S. KALIRAI<sup>2</sup>, MICHAEL M. SHARA<sup>3</sup>, AARON DOTTER<sup>4</sup>,  
GREGORY G. FAHLMAN<sup>5</sup>, R. MICHAEL RICH<sup>6</sup>

as of July 4, 2018

### ABSTRACT

Based on the width of its main sequence, and an actual observed split when viewed through particular filters, it is widely accepted that 47 Tucanae contains multiple stellar populations. In this contribution, we divide the main-sequence of 47 Tuc into four color groups, which presumably represent stars of various chemical compositions. The kinematic properties of each of these groups is explored via proper-motions, and a strong signal emerges of differing proper-motion anisotropies with differing main-sequence color; the bluest main-sequence stars exhibit the largest proper-motion anisotropy which becomes undetectable for the reddest stars. In addition, the bluest stars are also the most centrally concentrated. A similar analysis for SMC stars, which are located in the background of 47 Tuc on our frames, yields none of the anisotropy exhibited by the 47 Tuc stars. We discuss implications of these results for possible formation scenarios of the various populations.

*Subject headings:* globular clusters: individual (47 Tuc) — stars: Population II, Hertzsprung-Russell and C-M diagrams, kinematics and dynamics

### 1. INTRODUCTION

Previous to about 1980, the general paradigm for globular star clusters was that they were simple stellar populations, that is all stars had uniform chemical composition and were all the same age. However, since that time, numerous spectroscopic studies have shown that many of these clusters exhibit chemical composition variations among their stars likely caused by H-burning via the hot CNO cycle (see Gratton et al. 2004 for a nice review). Recent imaging observations with the Hubble Space Telescope (HST) that produced exquisitely precise photometry has extended this picture to many if not all clusters (see Piotto 2009 for a recent review). However, what is currently lacking is detailed insight into the manner of formation of the various stellar populations in such a cluster. Key input could potentially come from the observation of different dynamics or spatial distributions of the various populations. Sollima et al. (2007) did find radial variations among blue and red main sequence (MS) stars in  $\omega$  Cen, but this observation was not coupled with any proper motion (PM) information.

The MS of 47 Tuc is broader than observational error alone can explain. This was first pointed out by Anderson et al. (2009) and examined in some detail by Milone et al. (2012a) who clearly demonstrated that the CMD

width could be explained as a second-generation population, making up 70% of the total, enriched in both He and N and depleted in C and O.

Vesperini et al. (2013), using N-body simulations, have explored the behavior of first- and second-generation stars in a multi-population cluster. In general they find that complete mixing of the two populations does not occur until the cluster is well advanced dynamically; that is when it has lost upwards of 70% of its mass due to two-body relaxation. Giersz and Heggie (2011) performed a Monte Carlo simulation of 47 Tuc and concluded that it has likely lost only about 45% of its initial mass. We can thus expect that 47 Tuc's various populations will not yet be well-mixed and that it might be possible to observe either kinematic and/or spatial differences amongst its various stellar populations. Indeed there already exists a wealth of observations on the radial distributions of various stellar populations going back over 30 years (e.g. Norris and Freeman 1979, Milone 2012a) most of which suggest that stars exhibiting evidence for CN-enhancement are more centrally concentrated than CN-poor stars. Coupling this with kinematic observations could well provide critical clues to the multiple population scenario.

In § 2 below we discuss the observations relevant to the current study and follow this in § 3 with an exploration of the PM kinematics of cluster stars yielding strong evidence for differences amongst stars of differing MS colors (chemical compositions). § 4 presents a search for radial differences and § 5 discusses possible formation scenarios for the various stellar populations based on their currently observed motions and distributions.

### 2. THE DATA

Our team was awarded 121 HST orbits in Cycle 17 to image 47 Tuc (GO-11677). The main science goal was to obtain photometry with the ACS F606W and F814W filters that would go deep enough to study the entirety of the white dwarf cooling sequence. A detailed discussion of the observations can be found in Kalirai et al.

<sup>1</sup>Department of Physics & Astronomy, University of British Columbia, Vancouver, BC, Canada V6T 1Z1; richer@astro.ubc.ca, hey1@phas.ubc.ca

<sup>2</sup>Space Telescope Science Institute, Baltimore MD 21218; jayander@stsci.edu; jkalarai@stsci.edu

<sup>3</sup>Department of Astrophysics, American Museum of Natural History, Central Park West and 79th Street, New York, NY 10024; mshara@amnh.org

<sup>4</sup>Research School of Astronomy and Astrophysics, The Australian National University, Weston, ACT 2611, Australia; aaron.dotter@gmail.com

<sup>5</sup>National Research Council, Herzberg Institute of Astrophysics, Victoria, BC, Canada V9E 2E7; greg.fahlan@nrc-cnrc.gc.ca

<sup>6</sup>Division of Astronomy and Astrophysics, University of California at Los Angeles, Los Angeles, CA, 90095; rmr@astro.ucla.edu

(2012). We have supplemented these observations with F606W and F814W images in the archive taken between 2002 and 2012 with ACS/WFC and WFC3/UVIS. These images were taken at a very wide variety of offsets, orientations, and exposure times. Sources were found in each image independently and measured with a library PSF that had been constructed from other data sets (see Anderson and King 2006, AK06). Positions were corrected for distortion using the Bellini et al. (2011) solution for WFC3/UVIS and the AK06 solution for ACS, with an adjustment for the fact that the ACS solution has changed slightly since SM4.

We collated these many starlists in a reference frame based on that described in AK06. We identified the member stars from the CMD and used their positions in the reference frame and the individual frames to define a linear transformation from each 2048x2048-pixel amplifier into the reference frame. For each star, this gives us a reference-frame position for each exposure, and a linear fit can be made to this time series to compute the PMs and determine their errors. We iterated the procedure, which allowed us to do a better job of outlier rejection in the determination of the transformations. The result of this process is a list of average positions and PMs (and their errors) for each star in the list. Since the field was observed at a wide variety of pointings and orientations over  $\sim 10$  years, we would expect most minor issues such as errors in the distortion solution or errors in the pixel-based CTE correction to average out to zero and introduce only random errors, which would be reflected in our empirical PM-error estimates. We have validated this by computing local corrections for the reference-frame position of each star in each exposure based on the 25 closest stars within  $\pm 0.5$  magnitude of its brightness (as described in McLaughlin et al. 2006, and Anderson and van der Marel 2010). This strategy should remove any residual distortion or CTE errors. We find that the results of this local test are indistinguishable from those of our more global procedure.

The Small Magellanic Cloud (SMC) lies in the background of 47 Tuc. Fortunately the cluster is moving with respect to the SMC by several milliarcseconds (mas) per year, so that over the time span of all available images the differential motion of the two systems amounts to nearly a whole ACS pixel (50 mas) allowing us to separate out these populations via PMs.

Figure 1 displays the PM diagram for all stars in our frames. The 47 Tuc PM distribution was centered around (0,0) with the distribution centered near (4.5,1.5) for the SMC. We wanted to have as complete a sample as possible for both 47 Tuc and the SMC with a minimum of contamination. For this reason our PM cut was very generous, about  $10\sigma$  in each case. The left panel of Figure 2 presents the cluster CMD using all the stars on the frames detected with S/N > 30. We chose such a restrictive cut as our focus in this reduction is high-precision photometry and astrometry, so that is why the CMD does not penetrate to very faint magnitudes. The central panel contains the PM-selected sample. This PM-cleaned CMD allows us to determine the MS ridge line and, in addition, define a color and magnitude selected sample of stars whose magnitudes lie within the black box. The solid black circle in Figure 1 is the boundary of the PM sample for the SMC. We use both this PM

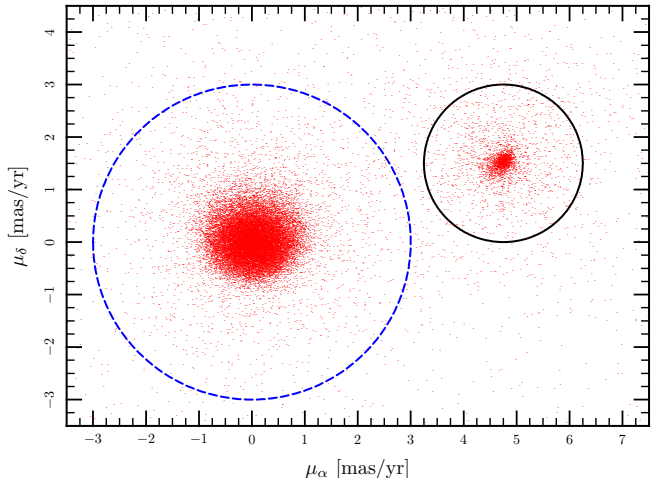


FIG. 1.— PMs of all stars in our frames. The large dashed blue circle encompasses the full 47 Tuc sample. The solid black circle is the boundary of the PM sample for the SMC.

selection and a color cut for the SMC sample in a similar manner.

### 3. PM KINEMATICS

We divide the 47 Tuc MS into four groups in color from bluest to reddest. We first sort the MS stars from brightest to faintest in F814W and divide this sorted sample into thirty non-overlapping groups of 800 stars each. For each group of stars we determine the median F606W – F814W color as well as the standard deviation of the distribution as estimated by the  $Q_n$  statistic (Rousseeuw & Croux 1991). As in Heyl et al. (2012) we use this statistic as a robust estimator of the standard deviation of a distribution, and we will denote its value by  $\hat{\sigma}$ . The right panel of Figure 2 displays the four color groups along the straightened MS of 47 Tuc as a function of apparent magnitude.

Thus we have defined the width through  $\hat{\sigma}$  and the center of the MS through the median as a function of F814W. By spline interpolation we determine the values of the width and median at the value of F814W for each star in the sample and assign each star to one of four color groups. The first group lies greater than one standard deviation and less than two standard deviations blueward of the median. The second group lies blueward of the median yet within one standard deviation. The third group lies redward of the median yet within one standard deviation. The fourth group lies more than one standard deviation and less than two standard deviations redward of the median. The PMs of all of the stars lie within the large circle in Figure 1, and their magnitudes lie within the box in Figure 2. The ridge line of the MS typically lies within the second group. The fourth group contains some binary stars with nearly equal mass components. Binaries with more unequal mass components lie closer to the MS ridge line. Chemical abundance variations can

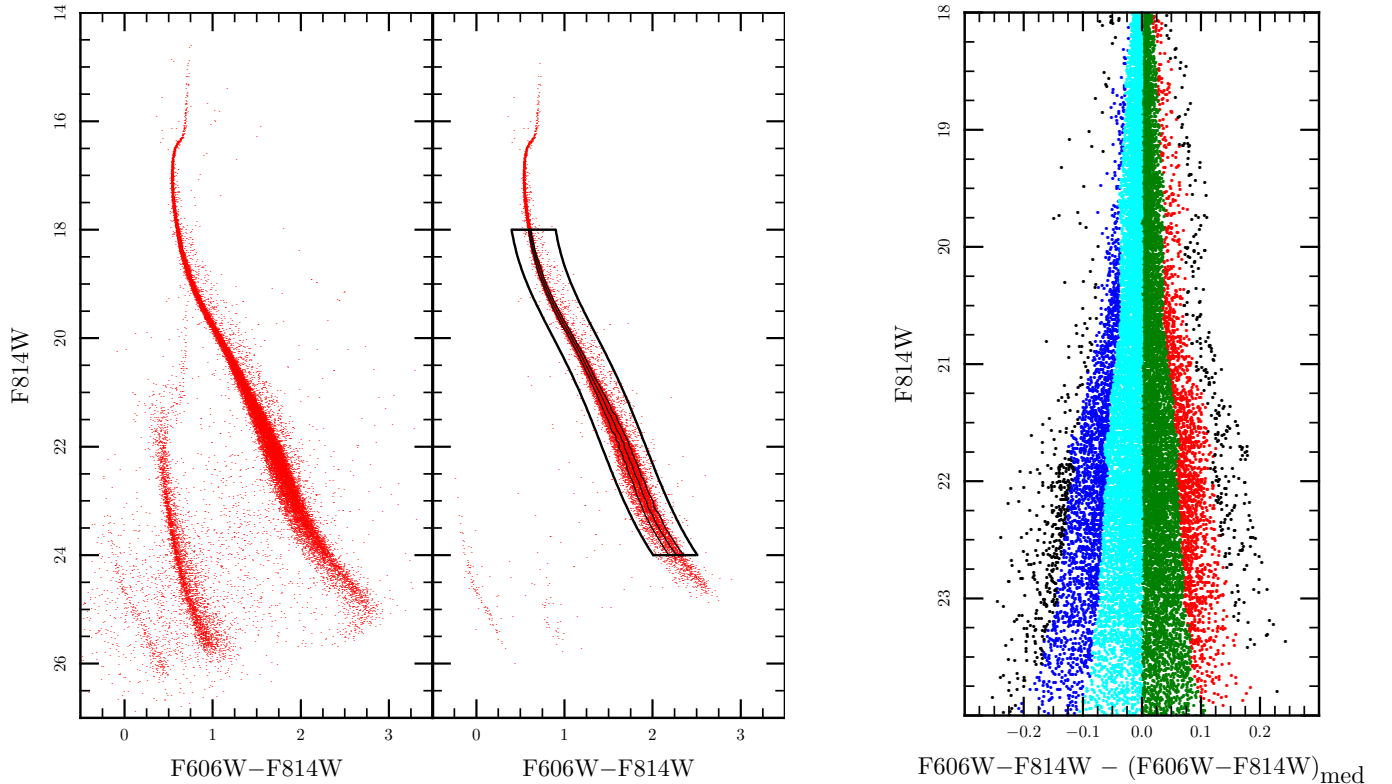


FIG. 2.— CMDs of 47 Tuc. Left: All objects detected in our 47 Tuc field (centered at 1.9 half light radii) with  $S/N > 30$ . Middle: The same data as in the left panel but now PM-cleaned to eliminate all but the 47 Tuc stars. Only the MS stars within the indicated box are retained for analysis. The light lines in this panel delineate the color groups outlined in § 3. Right: The straightened CMD indicating the four color groups used in the analysis. The black points at the color extremes were not used - they were more than two standard deviations away from the median color at a given magnitude.

also affect the color of single stars resulting in a spread in color. Our data are not sufficient to determine whether a particular stellar object is a single star with a peculiar chemical abundance, a binary or an optical double. Because the measured binary frequency for mass ratios greater than 0.6 in 47 Tuc is only a few percent (Milone et al. 2012b), the binaries will not significantly affect our results. These four color groups, indicated on the 47 Tuc CMD in the middle panel of Figure 2, presumably mostly represent stars of differing chemical composition with a small admixture of binaries.

Milone et al. (2012a) found in their analysis of the 47 Tuc MS that the various populations were often intertwined and crossed each other in the CMD. This was generally seen in the most ultraviolet filters which are much more sensitive to chemical composition variations than F606W and F814W used here. We tested whether He-enhanced MS stars at the metallicity of 47 Tuc were always bluer in color than He-normal stars at all luminosities by overlaying a series of models (Dotter et al. 2008) with various enhanced He compositions on the CMD. Over the entire extent of the MS explored in this paper, the He-rich MS remained blue-ward of the He-normal sequence. So we can be reasonably confident that the sequences of various abundances do not cross in the filters used here – the populations do not mix.

In Figure 3 (top) we plot the PM dispersions in the radial and tangential directions with respect to the cluster center for the four groups. In calculating these disper-

sions we have added an additional cut in the estimated PM error. We use only the stars whose errors are less than twice the median PM error at their apparent magnitude. The error bars in the dispersions denote 90% confidence regions as determined by bootstrapping the sample.

If the stars are moving isotropically, the dispersions in these two orthogonal directions should be the same. Clearly they are not. The anisotropy is largest for the bluest stars and reduces to no discernible anisotropy for the reddest ones.

This signature persists at all magnitudes. In Figure 4, we combine bins 1+2 and bins 3+4 and examine the dispersion of the blue and red stars as a function of magnitude, with 1000 stars in each magnitude bin. At all magnitudes, the dispersion of the blue stars in the tangential direction is always significantly smaller than their radial dispersion while for the red stars the dispersions exhibit little difference. The left-most set of points in this diagram are the median values of the proper motions of the blue and red stars for which there are no discernible trends.

As a sanity check, we carried out a similar analysis on the SMC stars. Again we divide the MS of the SMC into four color bins. Of course, since the MS of the SMC is much bluer than that of 47 Tuc, the SMC groups have different color ranges compared to those in 47 Tuc. We have restricted our sample here to lie below the turnoff of the SMC (fainter than  $F814W = 22$ ) and brighter than

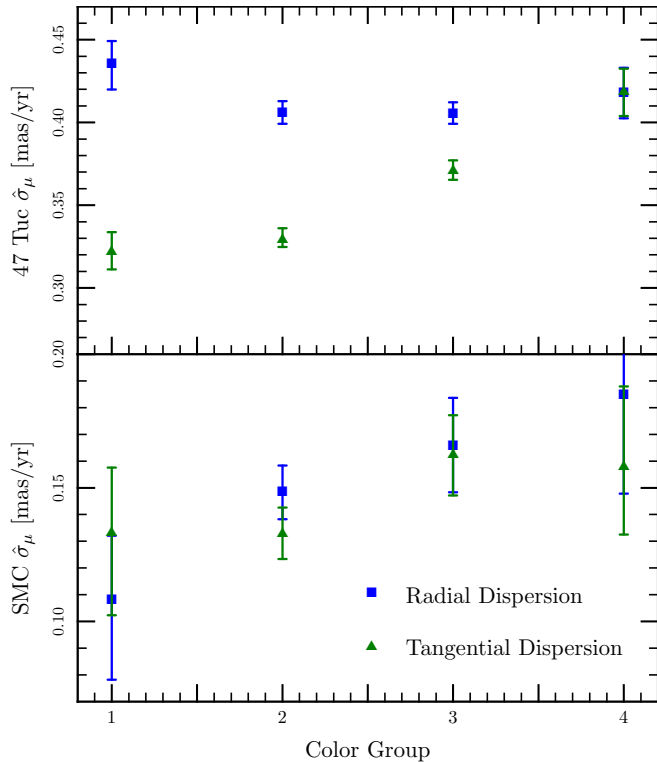


FIG. 3.— The radial and tangential PM dispersions as a function of color group (1 is the bluest MS group, 4 the reddest) for 47 Tuc (top) and the SMC (bottom).

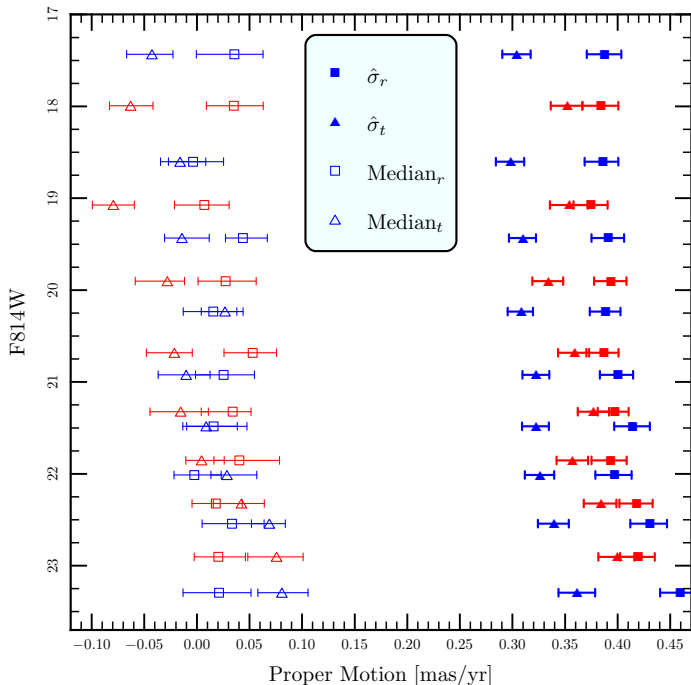


FIG. 4.— The PM median values (open symbols) and dispersions (filled symbols) in the tangential and radial directions as a function of magnitude for blue MS stars (groups 1 and 2 together) and the red MS stars (groups 3 and 4).

24 in F814W. We measured the PM dispersions along the same radial and tangential axes of the direction to the 47 Tuc center as a check on any potential systematic effects. Clearly these axes have no physical significance for the SMC. These dispersions with color group are illustrated in the bottom panel of Figure 3.

The PMs and their dispersions here are much smaller than in 47 Tuc reflecting mainly the SMC’s greater distance; it is twelve times farther from the Sun than is 47 Tuc. In contrast with 47 Tuc, there is no evidence for any anisotropy in these PMs.

#### 4. RADIAL EFFECTS

In addition to PM effects, we searched for radial differences among the various 47 Tuc color groups. Since 47 Tuc is at best barely relaxed, any discernible signals here could potentially provide important clues to formation scenarios of the populations. From KS tests of significance on the cumulative radial distributions of the various MS color groups, we find that the bluest group is less and less likely to be drawn from the same radial distribution as the other groups as we progress redward. A comparison of group 1’s with group 4’s distribution yields a probability of only  $2.80 \times 10^{-4}$  that these two distributions were drawn from the same parent sample. In these comparisons, the bluest group is always the most centrally concentrated. If the spread in MS color of 47 Tuc was due to a large contribution of binaries, one would expect that the reddest color bin would be the most centrally concentrated due to mass segregation of these heavier stars.

#### 5. DISCUSSION

The preceding analysis has shown that the 47 Tuc MS stars demonstrate anisotropic PMs that are strongly correlated with their colors. The sense of this result is that the bluest stars possess the most anisotropic motions (larger radial than tangential dispersions) while the reddest stars exhibit no measurable anisotropy. The motions of the SMC stars are completely consistent with no anisotropy along orthogonal axes towards and at right angles to the center of 47 Tuc. In addition, the bluer 47 Tuc MS stars are more centrally concentrated than the redder stars.

These differences contradict the notion that the globular cluster formed monolithically. Milone et al. (2012a) demonstrate that the blue cohort exhibits CNO processing and therefore likely He enrichment. This seems to firmly establish these stars as second generation.

What do we expect for the motions and radial distribution of this second generation of stars? Near the half-mass radius, 47 Tuc has gone through only three half-mass relaxation times and our field is near this radius. If the cluster is not yet relaxed at this radius, we would expect this second generation cohort to be more centrally concentrated, which it is. This is because these stars formed from dissipational gas expelled from massive first generation stars. Their current orbits are more radial as they are in the process of relaxing via two-body interactions to a distribution that is characteristic of their low masses - they are slowing diffusing outward (radially) to accomplish this.

The first generation stars exhibit no measurable anisotropy. This is not entirely easy to understand.

Whether they underwent violent relaxation before the second generation formed, or whether they still retain a memory of their initial collapse, they should still be on moderately radial orbits. This can be seen in Figure 4-21 of Binney and Tremaine (1987) where stars outside the central core region of a model cluster that underwent violent relaxation have anisotropic velocities at late times. However, the relaxation of the first generation of stars in 47 Tuc may be more complete because the initial state of the cluster may have been quite clumpy achieving more thorough relaxation (see e.g. Heyl et al. 1996) and not quasispherical as most simulations assume.

These broad-brushstrokes descriptions are illustrative only and not unique, but they do demonstrate how dynamical measurements could constrain the birth history of the cluster. Detailed numerical simulations including

gas dynamics would be required to get a clearer picture.

Based on observations with the NASA/ESA Hubble Space Telescope, obtained at the Space Telescope Science Institute, which is operated by the Association of Universities for Research in Astronomy, Inc., under NASA contract NAS5-26555. These observations are associated with proposal GO-11677. Support for program GO-11677 was provided by NASA through a grant from the Space Telescope Science Institute which is operated by the Association of Universities for Research, Inc., under NASA contract NAS5-26555. H.B.R. and J.H. are supported by grants from The Natural Sciences and Engineering Research Council of Canada and by the University of British Columbia. J.A., J.S.K., R.M.R and M.M.S. were funded by NASA. The authors benefited from useful conversations with Brett Gladman.

#### REFERENCES

- Anderson, J., & King, I. R. 2003, *AJ*, 126, 772  
 Anderson, J., & King, I. R. 2006, *Instrument Science Report ACS 2006-01*, 34 pages, 1  
 Anderson, J., King, I. R., Richer, H. B., Fahlman, G. G., Hansen, B. M. S., Hurley, J., Kalirai, J. S., Rich, R. M., & Stetson, P. B. 2008, *AJ*, 135, 2114  
 Anderson, J., & van der Marel, R. P. 2010, *ApJ*, 710, 1032  
 Bellini, A., Anderson, J., & Bedin, L. R. 2011, *PASP*, 123, 622  
 Binney, J., & Tremaine, S. 1987, Princeton, NJ, Princeton University Press, 1987, 747 p.,  
 Giersz, M., & Heggie, D. C. 2011, *MNRAS*, 410, 2698  
 Gratton, R., Sneden, C., & Carretta, E. 2004, *ARA&A*, 42, 385  
 Heyl, J. S., Hernquist, L., & Spergel, D. N. 1996, *ApJ*, 463, 69  
 Heyl, J. S., Richer, H., Anderson, J., et al. 2012, *ApJ*, 761, 51  
 Kalirai, J. S., Richer, H. B., Anderson, J., et al. 2012, *AJ*, 143, 11  
 McLaughlin, D. E., Anderson, J., Meylan, G., et al. 2006, *ApJS*, 166, 249  
 Milone, A. P., Marino, A. F., Piotto, G., et al. 2012a, *ApJ*, 744, 58  
 Milone, A. P., Piotto, G., Bedin, L. R., et al. 2012, *A&A*, 540, A16  
 Norris, J., & Freeman, K. C. 1979, *ApJ*, 230, L179  
 Piotto, G. 2009, *IAU Symposium*, 258, 233  
 Rousseeuw, P.J. & Croux, N.N. *Journal of the American Statistical Association* 88, 20, 1991  
 Sollima, A., Ferraro, F. R., Bellazzini, M., et al. 2007, *ApJ*, 654, 915  
 Vesperini, E., McMillan, S. L. W., D'Antona, F., & D'Ercole, A. 2013, *MNRAS*, 429, 1913